

THREE-DIMENSIONAL DISTRIBUTION OF INTERSTELLAR GAS IN DISK-SHAPED GALAXIES

HU WEN-BUI

(*Institute of Mechanics, Academia Sinica*)

ABSTRACT

In this paper, the three-dimensional structure of the large-scale interstellar gas under the action of the resultant gravitational field of stars and gas is discussed on the basis of the fundamental equations of gas dynamics. The galactic mass distribution and the kinetic characteristics of gas (such as the rotating curve...) being given, an exact solution of the spatial distribution of interstellar gas is obtained, and the peak distribution of gas in disk-shaped galaxies is discussed. The general features of galactic wing are analysed by using a momentum intergral, and the three-dimensional distribution of iso-pressure line of interstellar gas is calculated by using the Schmidt (1956) galactic model, and some possible tendencies of the galactic wing are pointed out. A general discussion about the origin of the high-velocity characteristic gaseous clouds in the galactic wing is also given.

I. INTRODUCTION

Based on the 21 cm surveys of both positive and negative galactic latitudes [1], it has been shown that the spiral arms extend in the direction perpendicular to the galactic plane. The average thickness of an arm is about 250 pc, but the outer arms have long "wings", which extend to at least 1 to 2 kpc in the perpendicular direction. It should be noted that these galactic wings have no tendency to merge into the more or less continuous halo, and seem to be connected to their originating arms [2]. The main characteristics of galactic wings can be summarised in these terms: beyond the sun, the neutral hydrogen connected with individual arms at a height of 1 to 2 kpc has a density equal to 1-2% of that in the plane [3]; further, characteristic clouds with large, negative radial velocities have been discovered in several localised regions in the galactic wings, which means that the gas density in the wings has considerable departure from axial symmetry. These characteristic, high-velocity clouds have been observed in the positive galactic latitudes, but so far not in the negative latitudes.

The study of galactic wings is essentially a problem in the three-dimensional distribution of interstellar gas, this means that we must construct galactic models with at least two components, the stars and the gas. Classical theories of galactic models mostly adopt a superposition of several mass ellipsoids, and then establish some relation between the galactic rotation curve and the mass distribution [4,5]. In these analyses, the gas is contained within a certain ellipsoid. It is then not possible to show clearly the characteristics of the large-scale structure of the gas. On the other hand, galactic models with a self-gravitating gaseous disk constructed so far are limited to the case of an infinitely thin disk [6,7], and do not deal with the three-dimensional structure of the interstellar gas. Neither have they discussed the effect of the stars' gravitation on the

gas distribution.

Based on the principles of gas dynamics, this paper discusses the galactic mass distribution and the effect of gas-dynamical characteristics on the three-dimensional distribution of the interstellar gas.

2. LARGE-SCALE STRUCTURE OF THE INTERSTELLAR GAS

Let us suppose that the large-scale properties of the gas can be described by Euler's equation for an inviscid fluid. Considering that the interstellar magnetic field is rather weak (averaging only about 3 μ G), we may for the moment neglect the effect of Lorentz force [8]. Thus, the equation of motion for the interstellar gas in a steady state is:

$$\text{grad}\left(\frac{v^2}{2}\right) - \mathbf{v} \times \text{rot } \mathbf{v} = -\frac{1}{\rho} \text{grad } p - \text{grad}(\varphi + \varphi_*), \quad (2.1)$$

where ρ , p , θ are respectively the gas density, pressure and gravitational potential, \mathbf{v} is its velocity, and the subscript * indicates the corresponding quantities of the stars. Equation (2.1) expresses the dynamical equilibrium of the gas under its own and the stars' gravitation. The self and the stellar gravitational potentials each satisfies its own Poisson equation:

$$\Delta\varphi = 4\pi G\rho, \quad (2.2)$$

$$\Delta\varphi_* = 4\pi G\rho_*, \quad (2.3)$$

where G is the gravitational constant and Δ is the Laplacian. In cylindrical coordinates, when there is axial symmetry,

$$\Delta = \frac{1}{\tilde{\omega}} \frac{\partial}{\partial \tilde{\omega}} \left(\tilde{\omega} \frac{\partial}{\partial \tilde{\omega}} \right) + \frac{\partial^2}{\partial z^2}.$$

If we put $\varphi_t = \varphi + \varphi_*$, $\rho_t = \rho + \rho_*$, then the total potential should satisfy the relation

$$\Delta\varphi_t = 4\pi G\rho_t. \quad (2.4)$$

Taking divergence of (2.1), we have

$$\text{div}\left(\frac{1}{\rho} \text{grad } p\right) = -4\pi G\rho_t - \Delta\left(\frac{v^2}{2}\right) + \text{div}(\mathbf{v} \times \text{rot } \mathbf{v}). \quad (2.5)$$

When there is axial symmetry,

$$\begin{aligned} & \text{div}(\mathbf{v} \times \text{rot } \mathbf{v}) - \Delta\left(\frac{v^2}{2}\right) \\ &= \frac{1}{\tilde{\omega}} \frac{\partial v_\theta^2}{\partial \tilde{\omega}} - \frac{1}{\tilde{\omega}} \frac{\partial}{\partial \tilde{\omega}} \left[\tilde{\omega} \left(v_\omega \frac{\partial v_\omega}{\partial \tilde{\omega}} + v_z \frac{\partial v_z}{\partial z} \right) \right] - \frac{\partial}{\partial z} \left(v_z \frac{\partial v_z}{\partial z} + v_\omega \frac{\partial v_\omega}{\partial \tilde{\omega}} \right), \end{aligned} \quad (2.6)$$

where $\tilde{\omega}$, θ , z are the cylindrical coordinates and v_ω , v_θ , v_z , the corresponding velocity components. Introducing the normal pressure relation* for a gas and denote

$$P(\rho) = \int \frac{dp}{\rho}. \quad (2.7)$$

*Translator's note: Author presumably means the assumption that ρ is a function of p only.

Putting (2.6) and (2.7) into (2.5), we obtain the relation among the gas density variation, the velocity field and the total density distribution,

$$\begin{aligned} \Delta P = & -4\pi G\rho_t + \frac{1}{\bar{\omega}} \frac{\partial v_\theta^2}{\partial \bar{\omega}} - \left\{ \frac{1}{\bar{\omega}} \frac{\partial}{\partial \bar{\omega}} \left[\bar{\omega} \left(v_\theta \frac{\partial v_\theta}{\partial \bar{\omega}} + v_z \frac{\partial v_z}{\partial z} \right) \right] \right. \\ & \left. + \frac{\partial}{\partial z} \left(v_z \frac{\partial v_z}{\partial z} + v_\theta \frac{\partial v_z}{\partial \bar{\omega}} \right) \right\}. \end{aligned} \quad (2.8)$$

For the usual spiral systems, we can take v_z to be much less than v_θ or v_θ , hence we can neglect the terms containing v_z in (2.8). We then have

$$\Delta P = -4\pi G\rho_t(\bar{\omega}, z) + \frac{1}{\bar{\omega}} \frac{\partial v_\theta^2(\bar{\omega}, z)}{\partial \bar{\omega}} - \frac{1}{2\bar{\omega}} \frac{\partial}{\partial \bar{\omega}} \left[\bar{\omega} \frac{\partial v_\theta^2(\bar{\omega}, z)}{\partial \bar{\omega}} \right]. \quad (2.9)$$

The boundary values at infinity of the gas pressure, density, and their gradients are all 0. The solution of (2.9) subject to these boundary conditions, is then,

$$\begin{aligned} P(\bar{\omega}, z) = & \int_{-\infty}^{\infty} \int_0^{\infty} \left\{ -4\pi G\rho_t(\xi, \zeta) + \frac{1}{\xi} \frac{\partial}{\partial \xi} v_\theta^2(\xi, \zeta) \right. \\ & \left. - \frac{1}{2\xi} \frac{\partial}{\partial \xi} \left[\xi \frac{\partial}{\partial \xi} v_\theta^2(\xi, \zeta) \right] \right\} \cdot G(\bar{\omega}, z; \xi, \zeta) d\xi d\zeta, \end{aligned} \quad (2.10)$$

where $G(\bar{\omega}, z; \xi, \zeta)$ is the fundamental solution of the two-dimensional Laplace equation in cylindrical coordinates for the case of axial symmetry; it is equal to

$$G(\bar{\omega}, z; \xi, \zeta) = \frac{\xi}{2\pi} \int_0^\pi \frac{d\alpha}{\sqrt{(\bar{\omega} - \xi)^2 + (z - \zeta)^2 + 4\xi\bar{\omega}\sin^2\alpha}}; \quad (2.11)$$

or it can be expressed as

$$\begin{aligned} G(\bar{\omega}, z; \xi, \zeta) = & \frac{1}{2\pi} \frac{\xi}{\sqrt{(\bar{\omega} + z)^2 + (z - \zeta)^2}} \int_{-\infty}^{\infty} \frac{dt}{\sqrt{(1-t^2)(k^2+t^2)}}, \\ & k^2 = \frac{(\bar{\omega} - \xi)^2 + (z - \zeta)^2}{(\bar{\omega} + \xi)^2 + (z - \zeta)^2}. \end{aligned}$$

Inserting into (2.10) the distributions of ρ_t , v_θ and v_ω , we can obtain the three-dimensional distribution of the gas density.

We now use a method in dynamics to simplify the analysis of the problem. In a self-contained dynamical theory, ρ_t and \mathbf{v} are closely bound up with the gas density ρ . We can make use of the available observational data and regard the total mass distribution ρ_t and the velocity field \mathbf{v} as known functions. This method of treatment greatly simplifies the solution of the problem; at the same time it enables us to discuss certain features in the large-scale structure of the gas.

Using (2.9) and (2.10), we can carry out some general discussions on the gas density distribution. Let us write out a specific normal pressure relation,

$$p = K\rho^\gamma, \quad (2.12)$$

where K and γ are both positive constants. From (2.7), we have

$$P(\rho) = \frac{K\gamma}{\gamma - 1} \rho^{\gamma-1}. \quad (2.13)$$

Our discussion will be limited to the case $\gamma > 1$, since, for $\gamma < 1$, instability may arise [9]. As may be seen from (2.13), $P(\rho)$ then varies in the same sense as the gas density. Since the Laplacian is a linear operator, we can write (2.9) as three separate Poisson equations, namely,

$$\Delta P_1 = -4\pi G\rho_t, \quad (2.14)$$

$$\Delta P_2 = \frac{1}{\tilde{\omega}} \frac{\partial}{\partial \tilde{\omega}} (v_\theta^2), \quad (2.15)$$

$$\Delta P_3 = -\frac{1}{2\tilde{\omega}} \frac{\partial}{\partial \tilde{\omega}} \left[\tilde{\omega} \frac{\partial}{\partial \tilde{\omega}} (v_z^2) \right], \quad (2.16)$$

with

$$P = P_1 + P_2 + P_3.$$

Given suitable boundary conditions, it is possible to solve for P_1 , P_2 , P_3 . Usual galactic model calculations all suppose that gravitation balances centrifugal force of the differential rotation and that galactic mass distribution is connected to the gravitational potential through the Poisson equation. From the dynamical point of view, P_1 corresponds to the part of the gas density distribution caused by the total mass distribution of the system (the total gravitation), P_2 is that caused by the galactic differential rotation, P_3 , that arising from the radial motions of the system, while the total P is the gas distribution corresponding to the given mass distribution and velocity field. These will now be discussed separately under the specific conditions of the Milky Way system.

1. About P_1 In (2.1), if we consider the static problem, then $\mathbf{v} = 0$. In this case, we have the static equilibrium relation

$$\Delta P = -\Delta\varphi_t = -4\pi G\rho_t. \quad (2.17)$$

or

$$\text{grad } P = -\text{grad } (\varphi_t),$$

Thus, P_1 is simply the usual mechanical potential, and is equal to the negative of the gravitational potential for a motionless system. Under the more general dynamical conditions ($\mathbf{v} \neq 0$), although (2.17) is the same as (2.4) and (2.14), P_1 and ϕ_t have different boundary values.

We know from observed data of the Milky Way that, on a large scale, the total mass density of the system is a monotonic, non-increasing function of $\tilde{\omega}$ and z . Thus, according to the property of the Poisson equation, P_1 will decrease with increasing $\tilde{\omega}$ and z . Equation (2.13) then shows that the gas density will, correspondingly, be a monotonic, non-increasing function of $\tilde{\omega}$ and z . The P_1 -distribution thus causes the gas density to be a maximum at the galactic centre and to decrease monotonically in all directions. This is directly opposite to the state of distribution of ϕ_t .

2. About P_2 As we are treating the problem dynamically, the equilibrium between

pressure gradient on one hand and the gravitation and inertial acceleration of the system on the other can be decomposed into a partial pressure gradient balancing the system's gravitation, another partial pressure gradient balancing the inertial forces due to tangential velocities, and a third partial pressure gradient balancing the inertial forces due to radial velocities. These three partial pressure gradients separately correspond to those of P_1 , P_2 , and P_3 , while their sum, $\text{grad } P$, is the pressure gradient for unit mass.

There are now fairly good observations of the rotational curve of the gas in the Milky Way system (see fig. 1). The results show that near the centre ($\bar{\omega} < 1$ kpc), v_θ rapidly increases;

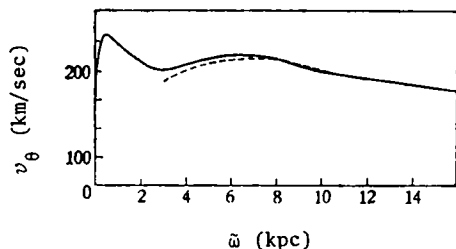


Fig. 1 Rotation Curve of the Milky Way [10] Dotted line shows the observed results in the southern hemisphere. Solid line is the rotation curve for the Northern hemisphere; the part inside the solar orbit is from observations, while the part outside is calculated from Schmidt's (1956) model.

in the main region of the spiral arms, it essentially keeps to a constant value, while beyond the orbit of the sun, it gradually decreases. Hence the RHS of (2.15) has a large extremal value somewhere near the centre and then gradually decreases: it is positive within the extreme value and is, on the whole, a small negative value beyond. Such a source function necessarily demands P_2 to have a rapid decrease near the centre, followed by a gradual increase over most of the outer regions.

3. About P_3 Spiral systems usually have comparatively small radial motion. However, explosions in the galactic nuclei can create

extremely high radial (and possibly axial) velocities in the central region. In the Milky Way system, phenomena such as the expansion of the 3-kpc arm are closely related to exploding activities of the nucleus. The effect of these high radial velocities on the distribution of gas density will show up in the central region.

Observations of the Milky Way system show that, between 1 and 4 kpc, the radial velocity $v_{\bar{\omega}}$ decreases with increasing $\bar{\omega}$, it is about +53 km/s at 3.7 kpc and generally does not exceed 15 km/s in the outer regions. This results in the RHS of (2.16) following first a negative then a positive variation, and thereby P_3 increases in the more central portions, and gradually decreases in the outer parts.

4. Combining the effects of P_1 , P_2 and P_3 . Adding together P_1 , P_2 and P_3 , we get the law of change of P . Although the mass distribution in the Milky Way system demands that the gas density take an extremal value at the galactic centre ($\bar{\omega} = 0$) and then monotonically decrease, the rotational motion causes the peak value of the gas density to move outwards to larger galactocentric distances, while the radial motion of the gas also produces some effect. This is in agreement with observations. The above analysis applies not only to the Milky Way system, but also to spiral systems in general.

In the first term on the right of (2.9), ρ_t is the sum of the gas and star densities. Separating the two, (2.9) can be re-written as

$$\Delta P + 4\pi G \left(\frac{\gamma - 1}{K\gamma} \right)^{\frac{1}{\gamma-1}} P^{\frac{1}{\gamma-1}} = -4\pi G \rho_* + \frac{1}{\bar{\omega}} \frac{\partial v_\theta^2}{\partial \bar{\omega}} - \frac{1}{2\bar{\omega}} \frac{\partial}{\partial \bar{\omega}} \left(\bar{\omega} \frac{\partial v^2}{\partial \bar{\omega}} \right). \quad (2.18)$$

Equation (2.18) is the relation between the star mass distribution and the density distribution of the gas in motion. It is a quasi-linear equation in P , the non-linear term is of the zeroth. For suitable boundary conditions, the solution of (2.18) exists and is unique. When $\gamma = 2$, (2.18) becomes linear. When $\gamma \neq 2$, we can generally carry out a numerical calculation by iteration.

3. PROPERTIES OF GALACTIC WINGS

When we have introduced into (2.10) the ascertained mass and velocity distributions, we can obtain the three-dimensional structure of the gas and then explaining certain features of the galactic wings. However, observational data cannot as yet provide a sufficiently good three-dimensional velocity field or mass distribution, and this makes an application of (2.10) difficult. In tackling this problem, we shall therefore start with a momentum integral. While this method is, in a certain sense, an approximation, it can provide a qualitative picture. To do this, we first discuss the following momentum integral.

For an ideal gas in steady state, if $\mathbf{v} \times \text{rot } \mathbf{v}$ is irrotational, i.e., if

$$\mathbf{v} \times \text{rot } \mathbf{v} = \text{grad } \chi(\tilde{\omega}, \theta, z), \quad (3.1)$$

then on inserting the conditions (2.7) and (3.1) into the equation (2.1), we get the momentum integral

$$\frac{v^2}{2} - \chi + \varphi + \varphi_* + P(\rho) = \text{const.} \quad (3.2)$$

Under the conditions in a disk-shaped galaxy, the interstellar gas approximately satisfies this momentum integral. If we do not consider the radial expansion in the central region, then for most parts of the system the velocity field can be regarded as directed in the tangential direction, i.e.,

$$\mathbf{v} = v_\theta \mathbf{e}_\theta,$$

where \mathbf{e}_θ is the unit vector along the tangent. We then have

$$\mathbf{v} \times \text{rot } \mathbf{v} = \text{grad} \left(\frac{v_\theta^2}{2} \right) + \frac{1}{\tilde{\omega}} v_\theta^2 \mathbf{e}_r, \quad (3.3)$$

where \mathbf{e}_r is the unit vector in the radial direction. Since the gas layer in the disk-shaped system is very thin, and the whole disk is located inside an extremely tenuous gas, the variation of v_θ with z is very slow, so we can take, approximately,

$$v_\theta = v_\theta(\tilde{\omega}). \quad (3.4)$$

Putting this in (3.3), we have

$$\mathbf{v} \times \text{rot } \mathbf{v} = \text{grad} \left[\frac{1}{2} v_\theta^2 + \frac{\partial}{\partial \tilde{\omega}} \left(\frac{v_\theta^2(\tilde{\omega})}{\tilde{\omega}} d\tilde{\omega} \right) \right]. \quad (3.5)$$

This shows that the assumption (3.4) will make $\mathbf{v} \times \text{rot } \mathbf{v}$ irrotational, thereby actually satisfying the condition for (3.1). On inserting (3.5) into (3.2), we now obtain the momentum integral

Translator's Note: In (3.5), $\frac{\partial}{\partial \tilde{\omega}}$ is presumably a misprint.

$$P(\rho) + \varphi + \varphi_* - \int \frac{1}{\tilde{\omega}} v_\theta^2(\tilde{\omega}) d\tilde{\omega} = \text{const.} \quad (3.6)$$

Both (3.2) and (3.6) are relations among local, not global, quantities. The approximate assumption (3.4) means that the integral relation (3.6) is a better approximation in regions far from the galactic nucleus than in the nucleus.

We now use (3.6) to discuss, in concrete terms, the structure of galactic wings and to analyse the form of iso-density lines. For $\rho = \text{const.}$, (3.6) gives

$$\varphi + \varphi_* = \int \frac{1}{\tilde{\omega}} v_\theta^2(\tilde{\omega}) d\tilde{\omega} + \text{const.} \quad (3.7)$$

In the $(\tilde{\omega}, z)$ plane, (3.7) represents a family of curves; in the $(\tilde{\omega}, \theta, z)$ space, it represents a family of surfaces of rotation, over each of which the gas density keeps to a constant value.

1. General Features of Galactic Wings

Since (3.7) relates local quantities, the rather complicated functional relation between the gravitational potential and the rotation curve can be developed into suitable Taylor series, separately for different regions, we thus approach the system piecewise, and obtain the large-scale features of the whole system by summation.

Let

$$\begin{cases} v_\theta = v_0 \left(\frac{\tilde{\omega}}{\tilde{\omega}_0} \right)^l, \\ \varphi_l = \varphi + \varphi_* \\ = -\varphi_0 \left[\left(\frac{\tilde{\omega}}{\tilde{\omega}_0} \right)^m + \left(\frac{z}{z_0} \right)^n + a \right]^{-1}, \end{cases} \quad (m \geq 0, n \geq 0, a > 0) \quad (3.8)$$

where z_0 and $\tilde{\omega}_0$ are characteristic scale-lengths, v_0 and θ_0 are characteristic velocity and potential, a, l, m, n are four appropriate parameters. For $\tilde{\omega}$ in an appropriate range, (3.7) can be written as

$$\varphi + \varphi_* = - \int_{\tilde{\omega}_s}^{\tilde{\omega}_t} \frac{1}{\tilde{\omega}} v_\theta^2(\tilde{\omega}) d\tilde{\omega} - c, \quad (3.9)$$

where $\tilde{\omega}_s$ is some reference radius, if θ_t and $P(\rho)$ at infinity are denoted respectively by θ_∞ and P_∞ , the constant c in the above equation can be expressed as

$$c = P(\rho) + \int_{\tilde{\omega}_s}^{\infty} \frac{1}{\tilde{\omega}} v_\theta^2(\tilde{\omega}) d\tilde{\omega} - \varphi_\infty - P_\infty. \quad (3.10)$$

Inserting (3.8) into (3.9), we get

$$\left(\frac{z}{z_0} \right)^n = \begin{cases} \frac{\varphi_0}{c + \frac{v_0^2}{2l} \left[\left(\frac{\tilde{\omega}_t}{\tilde{\omega}_0} \right)^{2l} - \left(\frac{\tilde{\omega}}{\tilde{\omega}_0} \right)^{2l} \right]} - \left(\frac{\tilde{\omega}}{\tilde{\omega}_0} \right)^m - a, & (l \neq 0) \\ \frac{\varphi_0}{c + v_0^2 \ln \left(\frac{\tilde{\omega}_t}{\tilde{\omega}} \right)} - \left(\frac{\tilde{\omega}}{\tilde{\omega}_0} \right)^m - a, & (l = 0) \end{cases} \quad (3.11)$$

(3.11) describes the form of iso-density lines for a certain range within the system. Of the

right side of (3.11), the first term is the main one that varies and we see from (3.8) that θ_0/a is the absolute value of the potential at the centre ($\bar{\omega} = 0, z = 0$), and therefore is a very large positive real number. It is known from general observational results that the rotational curve of a spiral system is such that, over a large part outside the nucleus, the linear velocity changes very slowly, slightly decreasing with increasing $\bar{\omega}$. Therefore, in (3.8), l is a very small negative number. This feature in the rotation demands the term in (3.11) containing θ_0 to be a slow, monotonically increasing function of $\bar{\omega}$. However, near the galactic centre, l is a fairly large positive number and the term containing θ_0 is expected to increase rapidly with $\bar{\omega}$. The second term on the right of (3.11), $-(\bar{\omega}/\bar{\omega}_0)^m$, is a monotonic, non-increasing function of $\bar{\omega}$, which reflects the way the potential varies with $\bar{\omega}$. Since the mass of a disk-shaped galaxy is concentrated in a very thin disk, we have $m \approx 0$ outside the disk, and $m > 0$ inside. Adding the results from the two parts, we see that the general tendency of an iso-density line is for z to increase with increasing $\bar{\omega}$, and this tendency is the greater the further out in the direction perpendicular to the galactic disk. Thus, the three-dimensional structure of the gas as reflected in the iso-density lines, actually shows certain features of the wings.

2. Structure of Galactic Wings

After obtaining the total mass distribution of the Milky Way system and the rotational curve of the interstellar gas through some means, we can calculate the form of the iso-density lines for the gas in the Milky Way system by using (3.6) or (3.9).

Observations show that the motion of the gas of the Milky Way system is quite complicated: there is a radial movement and the differential rotation is not completely axially symmetric. However, as an approximation to the large-scale aspect, we may elect to use such a rotational curve as given in Fig. 1. On the $(\bar{\omega}, z)$ plane a family of equipotential lines is constructed*, satisfying

$$\begin{cases} \varphi_i(\bar{\omega}, z) = c_i, \\ c_{i+1} - c_i = h = \text{const.} \end{cases} \quad (i = 1, 2, \dots) \quad (3.12)$$

Using the rotation curve given in Fig. 1, we seek a series of $\bar{\omega}$ values satisfying the following relations:

$$\begin{cases} - \int_{\bar{\omega}_i}^{\bar{\omega}} \frac{1}{\bar{\omega}} v_{\theta}^2(\bar{\omega}) d\bar{\omega} = c_i, \\ c_{i+1} - c_i = h = \text{const.} \end{cases} \quad (i = 1, 2, 3, \dots) \quad (3.13)$$

in which the values of c_i and h are the same as in (3.12). From this we can define a family of straight lines parallel to the z -axis in the $(\bar{\omega}, z)$ plane:

$$\bar{\omega} = \bar{\omega}_i, \quad (i = 1, 2, 3, \dots) \quad (3.14)$$

As (3.12) and (3.13) have the same step size h , the intersections of the family of curves (3.12) with the family of lines (3.13) will satisfy (3.9). Joining these points of intersection, two families of diagonals are obtained, of which one is such that each of its curves satisfies (3.9) with a constant value of c . This family of diagonals is the required family of iso-density lines. The smaller the chosen step length h , the more accurate will

* Using the numerical data in [11]. See Appendix I of this paper.

be the family of curves.

The results of a direct numerical calculation of (3.8) are shown in Fig. 2. The basic features of the iso-density lines of the gas are in accord with the foregoing discussion. Generally speaking, along an iso-density line, z increases with $\tilde{\omega}$; in regions near the nucleus where the inclination of the rotation curve is large, the iso-density lines have also large inclinations; in the middle range of galactocentric distance, $2 \text{ kpc} < \tilde{\omega} < 10 \text{ kpc}$ say, the iso-density lines near the galactic disk are rather flat, but their inclination increases with increasing z ; at large galactocentric distances where the potential changes essentially little, the inclinations of the iso-density lines tend to increase.

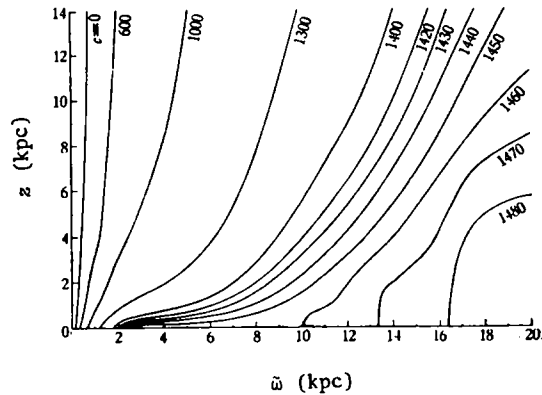


Fig. 2 Distribution of iso-density curves of the interstellar gas. The c -values are defined in (3.10), in units of 100 (km/s)^2 . $\tilde{\omega}_0 = 1 \text{ kpc}$ was used in the calculations.

In Fig. 2, we have marked the c -values as defined in (3.10) for the various curves. Since the gas pressure must be positive, we must have, according to the definition of c ,

$$P(\rho) = c + P_\infty + \varphi_\infty - \int_{\tilde{\omega}_0}^{\infty} \frac{1}{\tilde{\omega}} v_\theta^2(\tilde{\omega}) d\tilde{\omega} > 0. \quad (3.15)$$

As the centrifugal force integral term in (3.15) has a fairly large negative value, we require c to be not too small. Since larger c corresponds to higher pressure, Fig. 2 shows that, for a fixed galactocentric distance $\tilde{\omega}$, the pressure will decrease with increasing z , while for a given z , the pressure will increase with increasing $\tilde{\omega}$. If we consider that the position of the peak value of the gas density distribution has a rather large galactocentric distance, this then will accord with the observed tendency.

In the mathematical treatment of this section, we have introduced some simplifying assumptions, therefore we cannot regard Fig. 2 as giving an accurate three-dimensional structure of the gas distribution. Particularly in regions of small and very large $\tilde{\omega}$, where the gas motion is rather complicated, our simplifying assumptions regarding the flow field may not all hold, the actual iso-density curves may differ considerably from the calculated

ones. Nevertheless, for the main part of the Milky Way system, Fig 2 at least yields the general tendency of the gas structure, which tendency is in accord with the results observed so far, and has also a theoretical basis.

4. PROBLEMS CONCERNING THE HIGH-VELOCITY GAS CLOUDS

After this discussion of the large-scale structure of the interstellar gas, we now proceed to attempt an analysis of certain small-scale structure of the galactic wings, namely, problems concerning the high-velocity gas clouds. There have been many discussions on the high-velocity clouds outside the Milky Way plane. It is generally thought [12] that they originated in three possible ways, namely, (i) from supernova explosions outside the Milky Way plane; (ii) being extragalactic gas clouds that fall into our system, and (iii) from matter ejected from the galactic plane (e.g. explosions in the galactic nucleus) which then comes back to the plane. There is a large discrepancy between the kinematics of these clouds and their spatial distribution, which may be due to mechanisms that are not quite the same.

In the early stage of formation of the Milky Way system, its rotation may have been much faster than at present. At that time, more gas was gathered outside the galactic plane than is at present, and the iso-density curves of the galactic wings would have smaller inclinations. Part of the surplus gas could be the origin of the mass of the characteristic clouds now being observed [1]. According to (2.10), and neglecting the effect of $v_{\bar{\omega}}$, if v_{θ} were changed by a factor β while keeping to a similar velocity profile, then by and large, ρ_t will change by β^2 , hence also $P(\bar{\omega}, z)$. From (2.13) we then find that the gas density would correspondingly change by $\beta^{2/(\gamma-1)}$. If we take $\beta = 2$, then for $\gamma = 2$, the density would have been 4 times the present value, while for $\gamma = 1.5$, 2 times. Such high gas densities can provide a large amount of gaseous matter. In this way, we explain the origin of the high-velocity clouds in terms of the systems' own evolution, and we need not resort to an extragalactic source or exploding phenomena within the system.

The process of formation of the high-velocity clouds may be some mechanism of local instability. Interstellar magnetic fields may be very important in the small-scale dynamical processes in the Milky Way system. Many observations of the interstellar magnetic field of the Milky Way system have already been made. In the solar neighbourhood, the large-scale structure of the interstellar magnetic field is basically along the spiral arms, having a strength of about $3 \mu\text{G}$. There may also exist local fields with a spiral structure.

It is generally believed that many instability factors exist in the outer part of the galactic plane and in the space outside the plane. Although interstellar magnetic fields have a certain damping effect on the dynamical instability, it can hardly overcome Jeans' instability. The field itself also gives rise to some instabilities, particularly the Rayleigh-Taylor instability which may be important in forming isolated, locally dense clouds. We may also use this mechanism to explain the origin of the characteristic clouds of the galactic wings. According to Parker's theory, the localised, high-velocity clouds are the results of dynamical evolution during some billions of years; during this time, the gas gradually moved along the magnetic line and gathered in localised regions of low magnetic strength to form localised clouds of relatively high density.

During the condensation of gas into clouds, the local density of the gas gradually exceeded the local the local density in the large. Thus the "surplus" mass of the characteristic gas will destroy the original dynamical equilibrium, unless it is accompanied by the creation of a radial flow acceleration to compensate the gravitation between the "surplus" mass and the galactic matter, the bulk of which is the galactic disk. Therefore, as their mass increased, the clouds accelerated towards the galactic centre; but as the clouds moved towards the centre, their negative velocity also increased so as to maintain a negative acceleration. The negative radial velocities observed at present should vary continuously with time, the closer the cloud is to the centre, the greater will be the absolute value of its velocity. For the few localised clouds with positive radial velocities, we have to find some other explanation for their accelerating mechanism.

As compared to the high latitude regions, the middle latitude regions have greater gas density and the effect of a magnetic field there may also be more obvious. Thus the above explanation of the origin and motion of the high-velocity clouds is quite plausible for the mid-latitude regions. However, we must emphasize that it is not possible to use one and the same mechanism to account for both the origin and the motion of the high-velocity clouds.

I thank Comrade Pan Liang-ru for useful discussions in the course of the present work.

APPENDIX I POTENTIAL IN SCHMIDT'S (1956) MODEL III GALAXY

(units: $-100 \text{ km}^2/\text{s}^2$)

$\hat{\omega}(\text{kpc})$	0	2.05	3.075	4.100	5.125	6.150	7.175	8.200	9.225	10.250	11.275	12.300	14.350	16.400
0	1436	1012	869	748	644	554	475	410	358	318	285	258	217	188
0.1	1373	1003	864	745	642	553	475	410	358	318	285	258	217	188
0.2	1313	991	856	740	639	551	474	409	358	318	285	258	217	188
0.4	1208	959	834	725	630	544	470	407	357	317	285	258	217	188
0.7	1085	904	797	700	611	531	462	402	353	315	284	257	217	188
1.0	989	851	762	675	592	518	453	396	349	312	282	257	217	188
1.5	866	775	705	630	560	495	438	386	343	308	280	256	216	188
2	711	706	650	591	531	475	422	376	336	304	278	254	215	187
3	636	605	562	522	478	433	391	354	320	292	269	247	211	185
4	539	520	491	460	428	395	362	332	304	280	259	239	207	183
5	466	458	438	414	388	361	335	312	290	268	247	229	200	180
7	367	362	355	339	323	306	289	273	258	243	228	212	189	171
10	275	270	266	260	254	247	238	228	218	208	198	188	170	156
14	204	203	201	199	195	190	185	180	175	170	165	159		
18	160	160	159	158	156	154	152	150	148	145				

REFERENCES

- [1] Kepner, M., *Astron. Astrophys.*, 5 (1970), 444.
- [2] Oort, J. H., Survey of spiral structure problems, in *The Spiral Structure Of Our Galaxy* edited by: Becker, W. and Contopoulos, G., *IAU symp.*, no. 38 (1969), 1
- [3] Oort, J. H., Matter far from the galactic plane associated with spiral arms, *IAU symp.*, No. 38 (1969), 142.
- [4] Perek, L., *Advances in Astronomy and Astrophysics*, 1 (1962), 165.
- [5] Schmidt, M., Rotating parameters and distribution of mass in the Galaxy, in *Galactic Structure*. Edited by: Blaauw, A. and Schmidt, M., (1965), 513.
- [6] Toomre, A., *Astrophys. J.*, 138, 2 (1963), 385.
- [7] Hunter, C., *Monthly Notices R.A.S.*, 126 (1963), 299.
- [8] Lin, C. C., Theory of spiral structure, in *Galactic Astronomy*. Edited by: Chiu, H.Y. and Muriel, A., (1970), 18
- [9] Parker, E. N., *Astrophys. J.*, 145, 3 (1966), 811.
- [10] Kerr, F. J. and Westerhout, G., Distribution of interstellar hydrogen, in *Galactic Structure*, (1965), 172.
- [11] Schmidt, M., *B. A. N.*, 13, (1956), 15.
- [12] Oort, J. H., Radio astronomical studies of the Galactic System, in *Galaxies and the Universe*. Edited by: Woltjer, L. (1968), 1.